

Study of Wear and Friction of Al-Fe Metal Matrix Composite Produced by Liquid Metallurgical Method

A modified impeller mixing coupled with chill casting technique was used for the preparation of Al-Fe composite. The electrolytic grade iron powder of 300mesh size was dispersed in the melt of commercially pure aluminum. The iron content in the composite varied from 1.67 to 11.2 wt%. The presence of iron in the composite improved the ultimate tensile strength, 0.2% proof stress and the hardness. The ductility showed the adverse effect with increase of the iron content in the matrix. The results from microstructure showed the presence of second phase particles at the grain boundaries of aluminum-rich phase as well as within the grain itself which was confirmed by EPMA line as well as XRD analysis. These composite have also been subjected to wear and friction testing at different operating parameters. The XRD analysis was used to analyze the wear debris.

Keywords: Al-Fe composite, Liquid Metallurgy, wear, Friction, EPMA, XRD, UTS.

1. INTRODUCTION

The global energy crisis and depleting energy resources as well as stringent requirements of the quality of a product necessitated the development of lightweight energy efficient materials to be used in automotive industries [1-6]. The development of metal matrix composite with the dispersion of second phase particle had been catalyzed by the need for structural materials with high strength and stiffness to enhance the wear resistance [7-10].

Dispersoids exists in the form of particulates/fibers/whiskers, introduced into metal/alloy matrix either in the solids or in the liquid state whereby advantages of both matrix and reinforcements are obtained [11-15]. Currently titanium base alloys are used for aerospace application at elevated temperature [16]. But at the some places dispersion strengthened Al-base composite are being used for elevated temperature structural application up to 350°C. Such composite provides high strength at elevated temperature due

to formation of meta-stable intermetallic phases [17]. Formation of this intermetallic depends on processing route and selected parameter used in the fabrication.

Al-Fe intermetallics composite are of considerable importance because iron is invariably present as an impurity. Further these impurities are able to form different types of intermetallics [18-20]. In present work, Al-Fe composite are being produced by liquid metallurgical route and elevated mechanical, structural and tribological properties.

2. PREPARATION OF Al-Fe COMPOSITE

2.1 Selection of materials and procedure for preparation

Commercially pure aluminum (99.8%), electrolytic iron powder of 50 μm size was selected for the preparation of Al-Fe composites with different compositions.

The experimental set-up used for mixing and casting of composites is shown in Figure 1. It comprises of a cylindrical sillimanite crucible of 150mm diameter and 250mm depth with attachment of four baffles to its sidewalls for proper dispersion of second phase in melt during stirring. The crucible was placed in an

Sanjay Srivastava¹, Sunil Mohan²

¹Materials Science & Metallurgical Engineering
Maulana Azad National Institute of Technology,
Bhopal-462051

²Department of Metallurgy, Institute of Technology
Banaras Hindu University, Varanasi-221005
E-mail: s.srivastava.msme@gmail.com

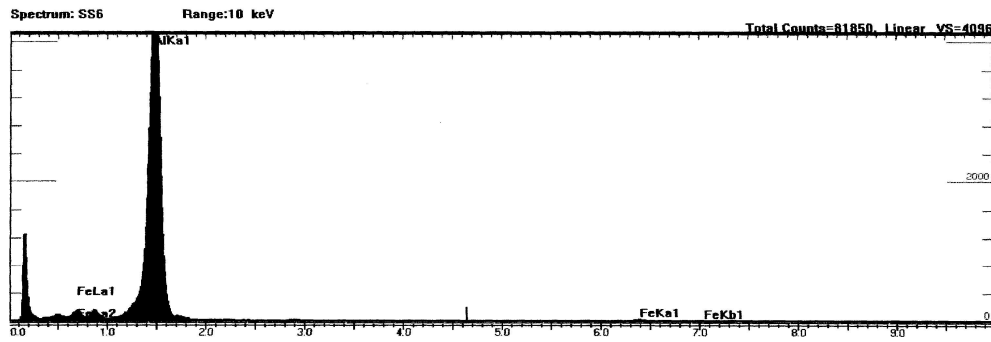


Figure 1. EDAX monograph of Al-6.23%Fe composite

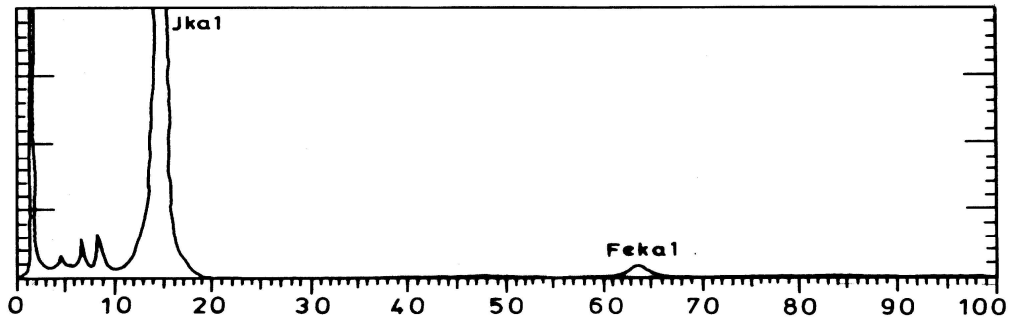


Figure 2. EDAX monograph of Al-11.2%Fe composite

electric heated muffle furnace. It was also equipped with a bottom pouring attachment, which could be closed or opened by graphite stopper with a lever system. A steel mould was placed beneath the furnace to cast the molten metal. In the top cover suitable opening was provided to charge materials and insert thermocouples. The temperature of the furnace could be controlled with an accuracy of about $\pm 5^{\circ}\text{C}$. Metallic bath temperature was measured continuously by chromel/alumel thermocouple. The agitator system could be raised or lowered with the help of the hanger and steel frame structure. After adjusting the mixer in a central position and required height from the bottom of the crucible, the motor was bolted and locked while mixing of melt. Three-blade impeller was used for effective mixing. This design provides very high rates of shear and only axial and radial flow currents are utilized for mixing without any significant vortex formation due to the presence of baffles. The Al-Fe composites were prepared employing liquid metallurgical route. The required amount of commercial pure aluminum was charged into the crucible and aluminum was heated to a temperature 200°C above its melting point i.e. 662°C . A mechanical stirrer was inserted into the melt, and agitation was started at a speed of 35 s^{-1} . The $50\text{-}\mu\text{m}$ -size electrolytic grade iron powder was charged into the melt during stirring and the

addition of the particulate into the melt was facilitated by vortex created by stirring action.

Mixing was done for a period of 60 seconds. The emulsion was poured into the chilled cylindrical mould placed beneath the crucible. The same procedure was adopted for different compositions. Cylindrical casting of length 20cm and dia.2cm were obtained.

2.2 Evaluation of as-cast Properties of the Composite

The wet chemical analysis was used to determine the percentage of iron in the bulk. The EDAX analysis was done as a confirmation test to iron presence.

EPMA has been used to trace the presence of iron which is either present at the grain boundary or within the grain of the composite. X-ray diffraction analysis was carried out for phase analysis.

The metallographic specimens were prepared using standard technique and studied under SEM for different feature present. The densities of the composite were determined using Archimede's principle. The hardness of the entire composite was measured using a Vickers hardness testing machine. The hardness was measured using Vickers hardness instrument Leitz Welzlar at a load of 5Kg. At least 3 indentations have been taken for each point. Tensile testing of all the Al-Fe composite

was performed stress along with percentage elongation and reductions in area were computed from the results.

2.3 Wear test

Pin-on-disc machine was used for evaluating the wear and friction properties under dry sliding condition. The cylindrical test pin of 8mm diameter and 40mm length were used against a hardened steel disc of 120 mm diameter. Tribological testing was conducted at varying sliding distances, applied loads and sliding velocities. In this experiment, the velocities were varied from 0.732m/sec to 3.82 m/sec and the loads were varying from 1Kg to 5Kg force.

Table 1 Chemical composition and Physical properties of Al-Fe composites

Composite	wt.% Fe	wt.% Al	Density (Theoretical) gm/cc	Density (Experimental) g/cc
Al-1.67% Fe	1.67	Remainder	2.79	2.63
Al-3.36% Fe	3.36	-do-	2.84	2.65
Al-6.23%Fe	6.23	-do-	2.96	2.79
Al-11.2%Fe	11.2	-do-	3.28	3.08

Further to confirm the presence of iron in the composites, energy dispersive X-ray analysis (EDAX) was also used. Figure 1 and 2 shows the EDAX monographs of composite with two different compositions. In these monographs larger peaks correspond to aluminum and smaller ones to iron. It confirms the presence of iron in the Al-Fe composite. The results were also confirmed with EPMA and EDAX analysis.

3.2 Physical analysis

Tables 1 show the physical properties of the different Al-Fe composites. It is observed from the table that the density increased from 2.79 to 3.08 as the iron content varied from 1.67 to 11.2%.

Table 2 Mechanical properties of the Al-Fe composite

S.No.	Composite	VHN	UTS(MPa)	0.2%PS(MPa)	% elongation
1	Al-1.67% Fe	95	142	59	32
2	Al-3.36% Fe	131	153	70	30
1	Al-6.23%Fe	163	159	74	27
2	Al-11.2%Fe	179	184	83	17

3.3 Metallographic Analysis

Figure 3a to 3d show the optical micrographs of composites with 1.67 to 11.2%Fe at different magnifications. These figures clearly reveal the presence of larger amount of second phase particles. These second phase particle exist in the

3. RESULT AND DISCUSSION

3.1 Chemical Analysis

Volumetric method is one of the most versatile techniques for the determination of element present at the microscopic level. In Al-Fe composites, iron is the minor constituent phase. Its percentage is determined by using the volumetric titration method.

Specimens from different sections were used to find out the uniformity of dispersion and results are tabulated in Table 1.

The mechanical properties of the composites are tabulated in Table 2. There is slight increase in the ultimate tensile strength (142 to 184MPa) 0.2% off-tensile stress (59 to 83MPa) as the iron content increased from 1.67 to 11.2% wt in the composite, providing a strengthening effect. However percentage elongation decreased from 32 to 17 with increase in the iron from 1.67 to 11.2wt. %.

Table 2 also shows the hardness values for all the four composites with different compositions. Hardness of the composites increases from 95 to 179 with increase in iron from 1.67 to 11.2%. The mechanical properties of cast aluminum are adversely affected by the presence of iron as large primary or pseudo-primary crystals [21, 22].

elongated form. These elongated forms appear in the needle shape at higher magnification and at the higher percentage of iron content. The needle shape intermetallic increases with increasing iron content. All the composites were also studied under SEM for further investigation the microstructures.

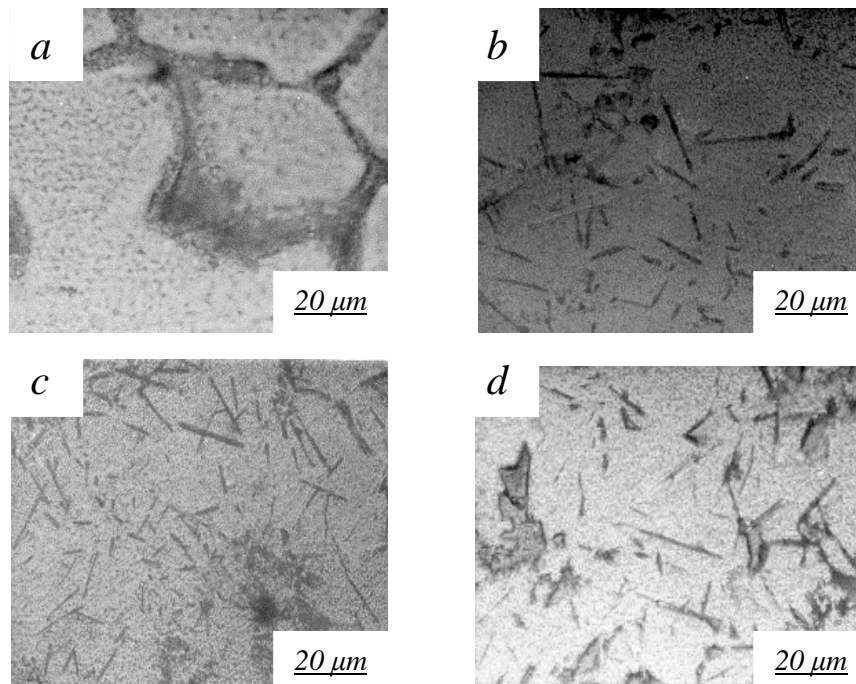


Figure 3. Optical micrographs of (a) Al-1.67%Fe (b) Al-3.36%Fe (c) Al-6.23%Fe (d) Al-11.2% Fe composite

Figure 4a to 4d shows the SEM micrographs of all the composites. At the lower magnification, clusters of Al-Fe intermetallics were seen, but at the high magnification, needle shape intermetallics were clearly visible. XRD analysis was conducted for all the four compositions produced with different iron

percentage. XRD monographs for different compositions are shown in Figure 5a to 5d for all composition of the selected composite materials. In these curves large peaks correspond to major phase aluminum and smaller one corresponds to FeAl_3 [23, 24].

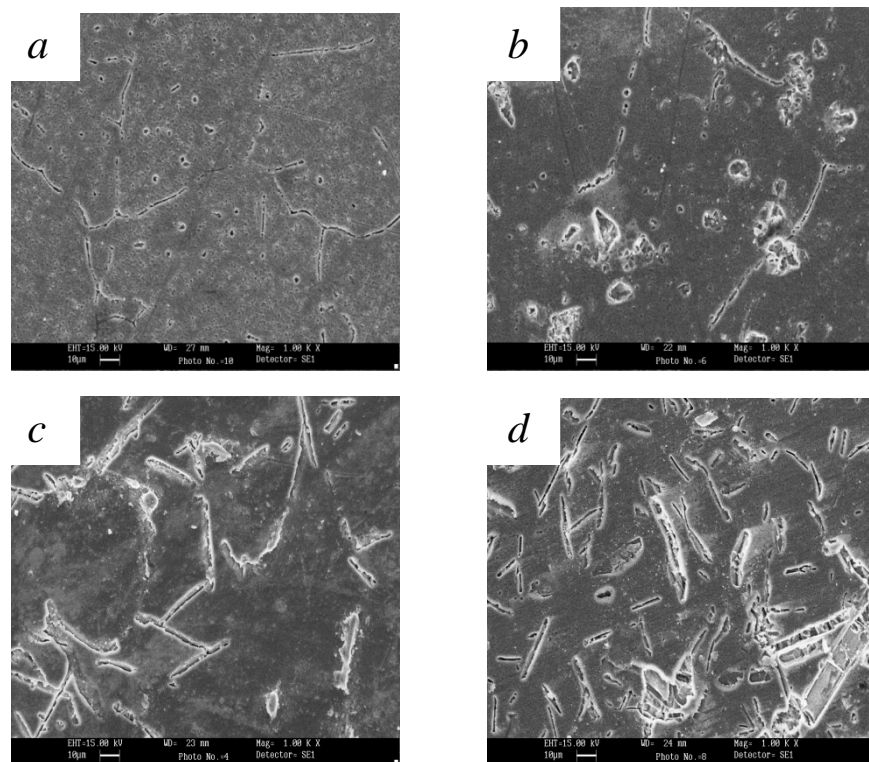


Figure 4. SEM micrographs of (a) Al-1.67%Fe (b) Al-3.36%Fe (c) Al-6.23%Fe (d) Al- 11.2% Fe composite.

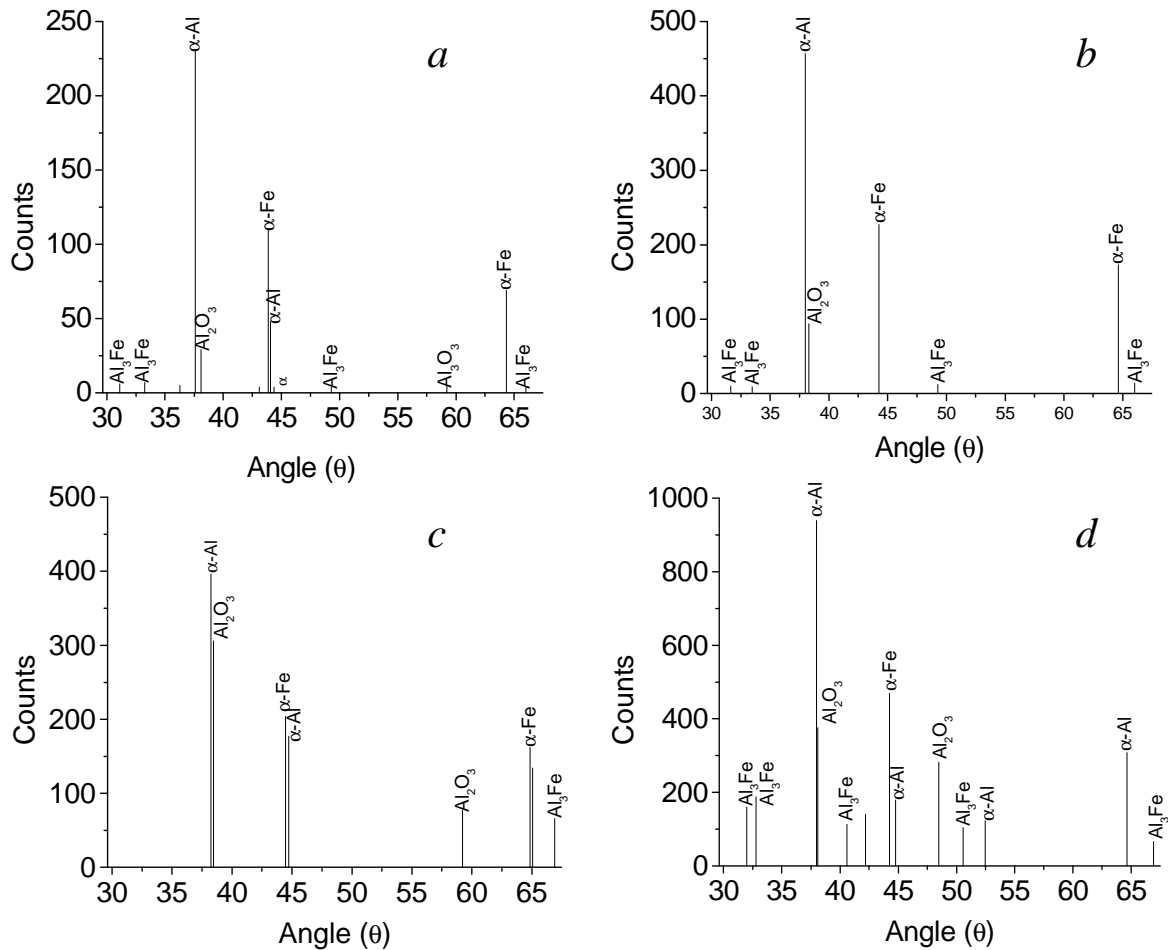


Figure 5. XRD graph of (a) Al-1.67%Fe (b) Al-3.36%Fe (c) Al-6.23%Fe (d) Al-11.2% Fe composite, showing presence of FeAl₃.

3.4 Wear studies

The variation of bulk wear with sliding distance was studied at different combination of loads and velocities. Figure 6 shows results for a test conducted at 0.37 MPa load and 0.772 m/s sliding velocity.

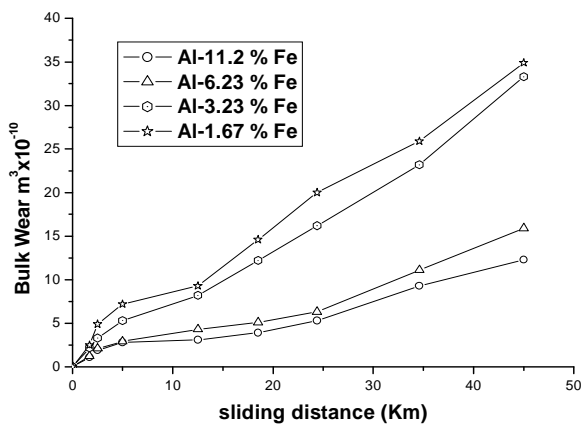


Figure 6. Variation of bulk wears with sliding distance at 3 kg load and 0.772 m/s sliding velocity for as-cast Al-Fe composites

It is seen that the initial running-in period is followed by steady state wear for all the composites. The bulk wear continuously decreases with increase in iron content. Steady state wear is observed after initial running-in period of 500-1000m in almost all the case irrespective of load or sliding velocity used. Al-11.2 %Fe showed lower bulk wear among all the composite which may be due to higher amount of hard phase formation increasing the overall hardness of the composite material. The relation found here is in accordance with the pattern for most metallic materials derived theoretically as well as observed experimentally [23,24]. However, at higher combination of load and sliding velocity bulk wear is higher for all four composite.

The studies conducted to see the effect of applied load on wear rate revealed that wear rate increased continuously with load in a linear manner irrespective of the sliding velocity[25,26] used as it is evident from Figure 7 at a particular velocity.

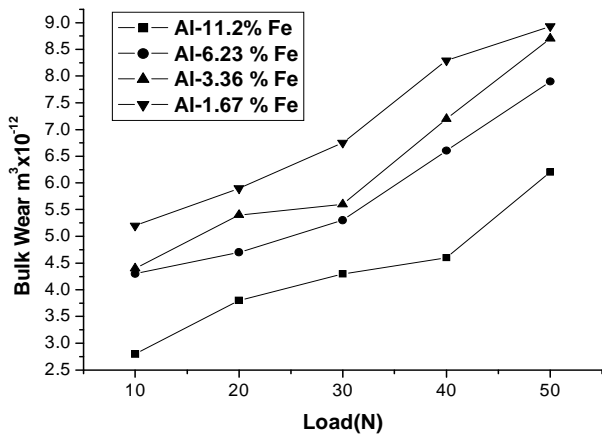


Figure 7. Variation of wear rate with load for Al-Fe composites

Figure 8 shows the variation of wear rate with sliding velocity at 1kg load. Like other aluminium alloys/composite, Al-Fe composite showed an initial decrease in wear rate followed by a sharp increase in wear rate after attaining minima in wear rate for all the composites at different loads. But in all the case wear rate decrease with increase in iron content for all combination of loads and sliding velocities used [27,28].

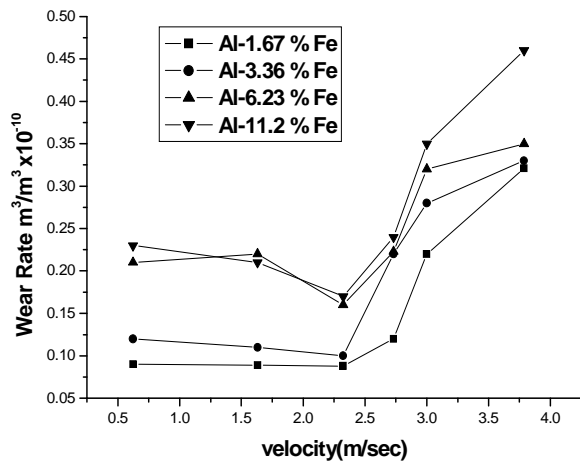


Figure 8. Variation of wear rate with sliding velocity at 1 kg load for Al-Fe composites

Figure 9 a and b shows the SEM study of the wear track of Al-11.2 wt% Fe at a different load. Wear debris are also examined with SEM. Debris of Al-Fe composite at a distance of about 1430m shows mainly oxidative nature and wear track is smooth with thin oxide layer, however at a distance of about 40000m debris comprised of different oxides with metallic particle and wear track was observed with thick oxide layer with deeper track as shown in Figure 9b. The mechanistic approach is changed with change the velocity and load. In this case the sliding distance was kept constant i.e., 4000m.

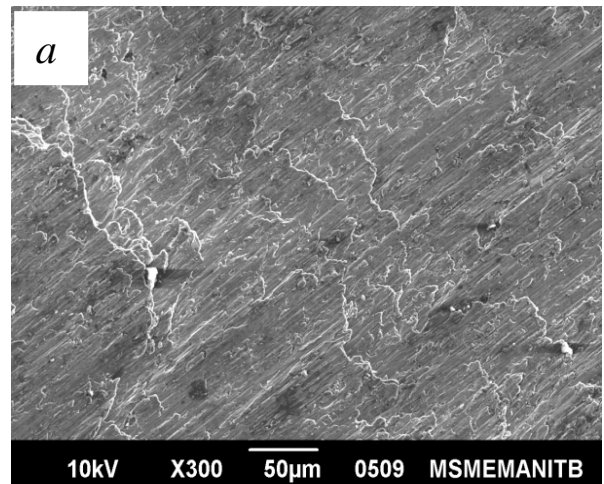
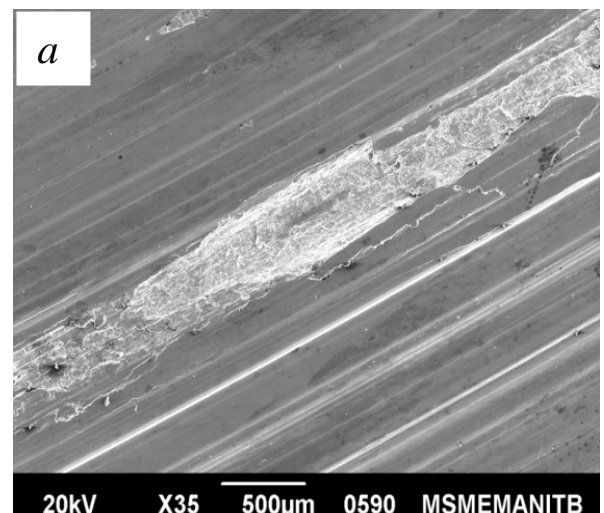


Figure 9. SEM micrographs of wear tracks of Al-11.2 wt. % Fe composite for 0.772 m/s sliding velocity and different sliding distance of (a) 1430m and (b) 4000m

Due to examination of wear track and debris as shown in the Figure 10a and 10b, the oxidative - metallic to metallic is observed as applied load and sliding velocity.



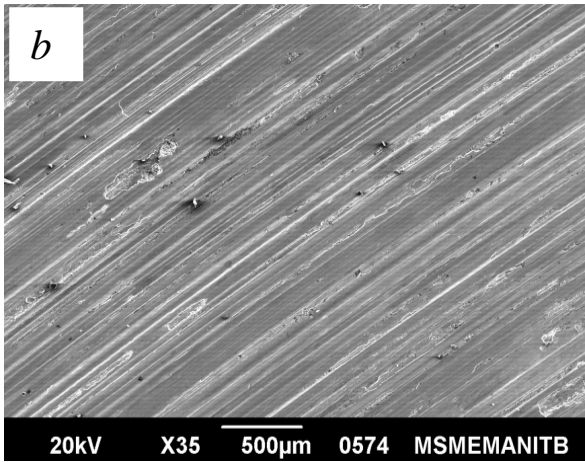


Figure 10. SEM micrographs of wear tracks of Al-11.2 wt. % Fe composite for 0.772 m/s sliding velocity and different loads of (a) 2.0 kg and (b) 5.0 kg.

The oxide film is broken at the higher velocity and load and deep groove and elimination of surface is observed as shown in Figure 11a and 11b.

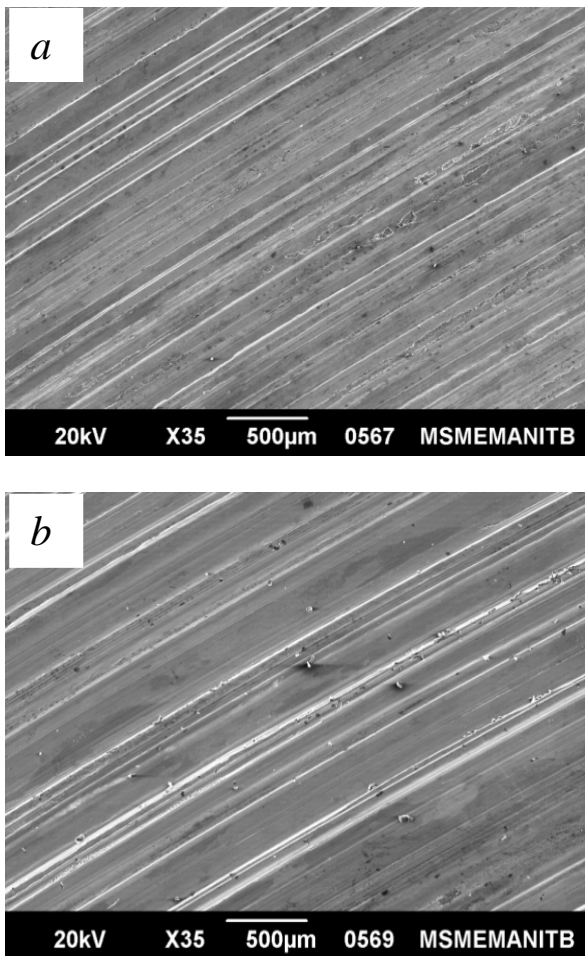


Figure 11. SEM micrographs of wear tracks of debris of Al-11.2 wt. % Fe composite for 3.24 m/s sliding velocity and different loads of (a) 2.0 kg and (b) 5.0 kg.

SEM images of the transverse section of the worn surface showed that the buildup of oxide layer depending on sliding distance, composition, applied load and sliding velocity. In mild wear region after large sliding distance cracking and spalling of oxide layer is observed on the wear track which turns into deep groove after large sliding distance for all Al-Fe composite. The higher percentage of oxide layer is formed in sample with lower iron content in comparison to the samples of higher Fe-content. The oxidation of the worn surface depends upon the hardness of the materials. The hardness of the materials varies with iron content in the materials. Al-11.2% Fe shows the maximum hardness and they have capability to sustain the load. This increases the bulk hardness of composite from 95 to 179 VHN with iron percentage increase from 1.67 to 11.2, hence improving the wear resistance of composites with increase in percentage iron for all case irrespective of load and sliding velocity.

XRD examination of wear debris shows the diffraction peaks corresponding to coexisting aluminum and alumina, different oxide of iron as well as the peaks of iron as shown in Figure 12. The main peak of the alumina are found at 37.6° (hkl: 213) and 37.8° (hkl: 109) and the different oxides of the iron at 33.18° and 35.46° . The peak of the iron is present at 44.67° [29-30].

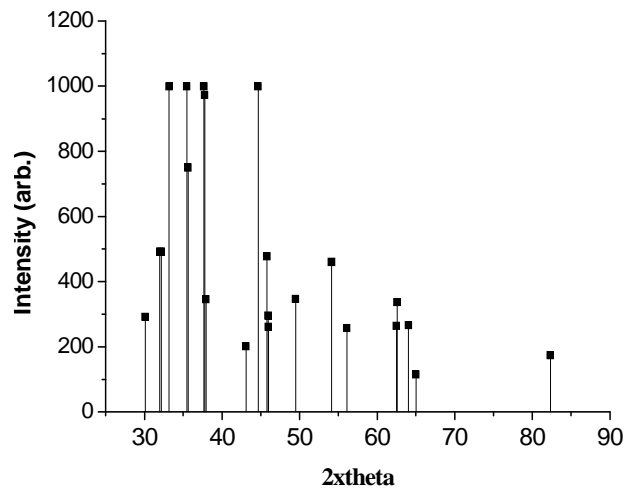


Figure 12. XRD plot of wear debris of Al-11.2 wt. % Fe composite at 0.772 m/s sliding velocity and 2.0 kg load.

3.5 Friction studies

The character of friction variation with sliding at the specific load (i.e. 10N) is illustrated in Figure 13. The Figure show is graphically representation of the results obtained from the friction experiment at a fixed load and sliding velocity. It is evident

from the Figure 13 the friction coefficient drastically decreases during the running in period. During the steady state period the friction coefficient is being stabilized. The friction behavior also varies with applied load.

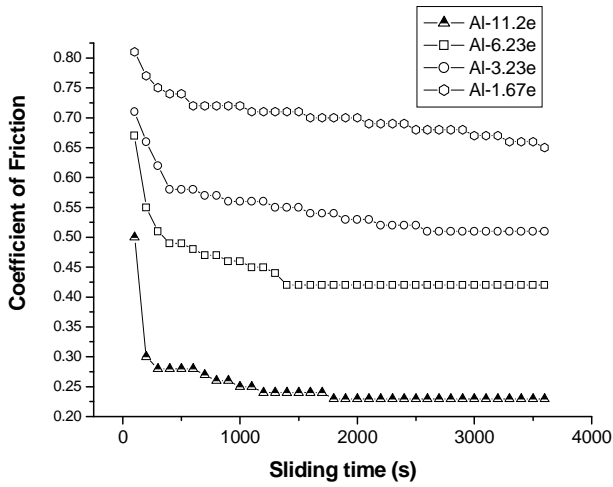


Figure 13. Friction coefficient variation of Al-Fe composite during sliding time at fixed specific loads (i.e 10N) and sliding speeds (4000m)

The average value of the friction coefficient at normal load is shown in Figure 14. In accordance with the figure the increase of the friction coefficient corresponds to increase the normal load. The increase rate is especially evident for load change from 15 to 30 N.

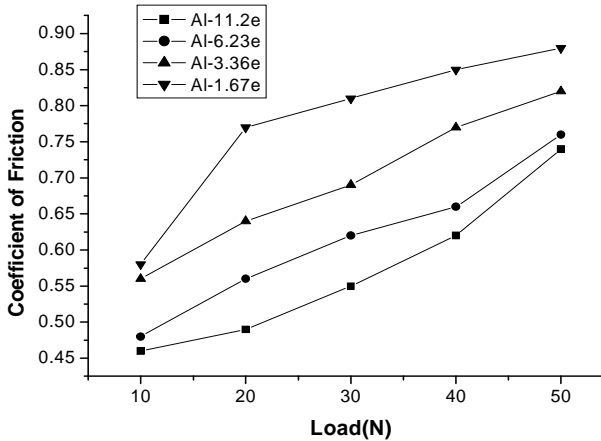


Figure 14. Coefficient of friction vs. applied load for Al-Fe composite at 0.932m/sec

Diagrams in Figure 15 show the dependence of the steady-state friction coefficient on the sliding speed, for various loads in dry sliding conditions. The nature of the dependence, in all the tested composite materials, manifests as decrease of the friction coefficient with increase of the sliding speed [31]. The degree of change is especially prominent in the region of lower values of speeds.

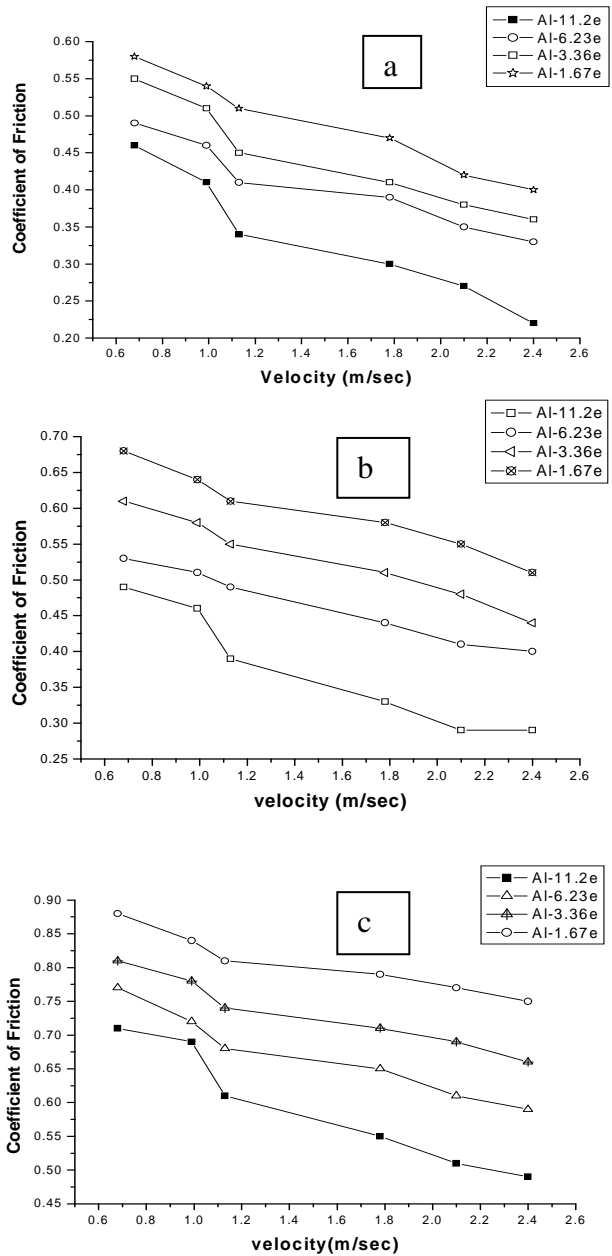


Fig15. Friction coefficient vs. sliding speed of Al-Fe composite at different applied loads: 10N (a), 20N (b), 50N (c)

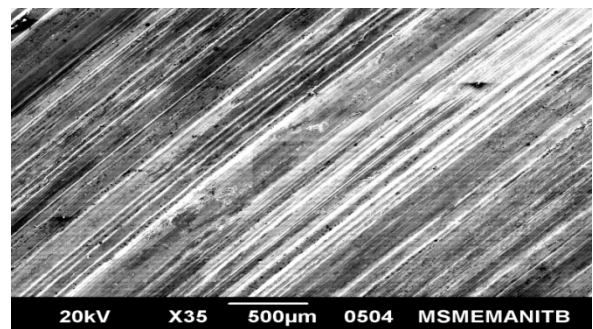


Figure 16. Worn surface of the Al-Fe composite tested in dry lubricated sliding condition for 50 N of applied load and 0.26 m/s of sliding speed during friction experiment.

The worn surfaces of the samples from the SEM examination are shown in Figure 16. The worn surfaces of the Al-11.2 wt% Fe samples were noticed to be smoother than those of the Al-1.67 wt% Fe. Generally, the parallel ploughing grooves and scratches can be seen over all the surfaces in the direction of sliding. These grooves and scratches resulted from the ploughing action of asperities on the counter disc of significantly higher hardness.

It can be noticed from the figure that for all the contact loads, the friction coefficient of Al-11.2%Fe is found to be low in comparison to the other the composites. Al-11.2 wt% Fe showed higher hardness and from the metallographic observation indicated is uniformly distribution of FeAl₃ within the composite. The iron intermetallic has higher hardness and also bear the maximum load. Therefore it acts as lubricant in the materials.

4. CONCLUSION

The Al-Fe composite is prepared from liquid metallurgical methods. It can be observed from the present investigation that iron could be successfully and uniformly distributed in aluminum using impeller mixing chill casting technique. UTS, 0.2%PS and VHN increased with increase the volume fraction of the iron in the matrix. The Al-11.2%Fe composite showed higher percentage of elongation while compared to Al-6.23% Fe. Finally the increase in iron content in the matrix supports the formation of different type of intermetallic. This intermetallic increased with volume fraction of iron in the matrix. Wear rate with sliding distance showed almost linear relationship for fixed load and sliding velocities. Wear rate of the composite materials initially decrease with sliding velocity and attains a minima in wear rate and then increases with further increase in sliding velocity.

REFERENCE

- [1] Mehrabian R., Riek R. and Flemings M. *Preparation and Casting of Metal-Particulate Non-Metal Composites*, Metall. Trans., 5, 1974, 1899-1905.
- [2] Lee C. S., Kim Y.H. and Han K.S and Lim T., *wear behavior of aluminum matrix composite materials*, J Mater Sci 27 (1992) 793.
- [3] Rohatgi P. and Asthana R., *Solidification Science in Cast MMCs: The influence of Merton Flemings*, JOM, 53, 9, 2001, 9-13.
- [4] Rohatgi P., *Cast Aluminum-Matrix Composites for Automotive Applications*, JOM, 42, 4, 1991, 10-15.
- [5] Prasad S.V, Rohatgi P. and Kosel T.H., *Mechanism of material removal during low stress abrasion of aluminum alloy-zircon particle composites*, Mater Sci and Engg 80 (1986) 213.
- [6] A. Uday, S. Dabada, Suhas Joshi, R.Balasubramaniam, V. V. Bhanu prasad., *“Surface finish and integrity of machined on Al/SiCp composites”*. Journal of Materials Processing Technology 192-193(2007) 166-174.
- [7] Das S., Prasad S.V., Ramachandran T. R., *Microstructure and wear of Cast(Al-Si)-Graphite composite*, Wear 133(1989)173.
- [8] Prakash U., Raghan T, Kamat S.V., and Gokhale A., *The effect of Mg-addition on microstructure and tensile and stress rupture properties of a P/M Al-Fe-Ce alloy*, Scripta Met 39 (1998) 867.
- [9] Mohan S., Prakash V., and Pathak J., *wear characteristics of HSLA-steel*, Wear 252(2002) 16-25.
- [10] Mohan S. and Srivastava S. *“Surface behaviour of as-Cast Al-Fe intermetallic composite”*. Tribology Letters, Vol.22, No.1, April 2006.
- [11] Hoskins F., Folgar Portillo F., Wunderlin R. and Mehrabian R., *Composites of Aluminum Alloys, Fabrication and Wear Behavior*, Journal of Materials Science, 17, 2, 1982, 477-498.
- [12] Jun D., Yao-hui L., Si-rong Yu and Wen-fang L., *Dry sliding friction and wear properties of Al₂O₃ and carbon short fibres reinforced Al-12Si alloy hybrid composites*, Wear, 257, 2004, 930– 940.
- [13] Korkut M.H., *Effect of particulate reinforcement on wear behavior of aluminum* 3838 Tribology in industry, Volume 26, No. 3&4, 2004. Matrix composites, Materials Science and Technology, 20, 1, Jan 2004, 73-81.
- [14] Prasad S.V. and Asthana R., *Aluminum metal-matrix composites for automotive applications: tribological considerations*, Tribology Letters, 17, 2004, 445-453.

- [15] Martin A., Martinez M.A. and LLorca J., *Wear of SiC-reinforced Al-matrix composites in the temperature range 20-200°C*, *Wear*, 193, 1996, 169-179.
- [16] Surappa M.K., *Aluminium matrix composites: Challenges and opportunities*, *Sādhanā*, 28, 1-2, 2003, 319-334.
- [17] Roy Debdas, Basu Bikramjit, Mallick Amitava Basu, Kumar B.V.Manoj and Ghosh Sumit, "Understanding the un lubricated friction in situ metal matrix composite". *Composite: Part A* 37 (2006) 1464-1472.
- [18] Park B.G., Ko S.H., Park Y.H. and Lee J.H., "Mechanical properties of in situ Fe₃Al matrix composites fabrication by MA-PDS process". *Intermetallics* 14 (2006) 660-665.
- [19] Prasad S.V., Asthana R., *Aluminum metal-matrix composites for automotive applications: tribological considerations*, *Tribology Letters*, 17, 3, 2004, 445-453.
- [20] Hunt W.H., Jr., Miracle D.B., *Automotive Applications of Metal-Matrix Composites*, in: D.B. Miracle, S.L. Donaldson (Ed.), *ASM Handbook, Volume 21: Composites*, ASM International, 2001, 1029-1032.
- [21] Mandolfo L. F., *Aluminum Alloys, structure and properties*, Butterworth's London (1976), 8585.
- [22] Narayanasamy R., Selvakumar N., and Pandey K. S., "Phenomenon of instantaneous strain Hardening behaviour of sintered Al-Fe composite performs during cold axial forming". *Materials and Design* 28 (2007) 1358-1363.
- [23] Zhang Yijie, Ma Naiheng, Yi Hongzhan, Wang S., and Wang H., "Effect of Fe on grain refinement of commercial purity aluminium" *Materials and Design* 27(2006)794-798.
- [24] Skrotzki W., Keegler K., Tamm R., and Oertel C.G., "Grain structure and Texture of cast iron aluminides" *Cryst. Res. Technol.*40, No.1/2, 90-94(2005).
- [25] García-Cordovilla C., Narciso J., Louis E., *Abrasive wear resistance of aluminum alloy/ceramic particulate composites*, *Wear*, 192, 1-2, 1996, 170-177.
- [26] Korkut M.H., *Effect of particulate reinforcement on wear behavior of aluminum matrix composites*, *Materials Science and Technology*, 20, 1, 2004, 73-81.
- [27] Zou X.G., Miyahara H., Yamamoto K., Ogi K., *Sliding wear behavior of Al-Si-Cu composites reinforced with SiC particles*, *Materials Science and Technology*, 19, 11, 2003, 1519-1526.
- [28] T. Miyajima, Y. Iwai, *Effects of reinforcements on sliding wear behavior of aluminum matrix composites*, *Wear*, 255, 1-6, 2003, 606-616.
- [29] S. Raadnui, *Wear particle analysis—utilization of quantitative computer image analysis: A review*, *Tribology International*, 38, 10, 2005, 871-878.
- [30] Foltz J.W., "Metal-Matrix Composites" in *ASM Handbook Vol. 2, Properties and Selection: Nonferrous Alloys and Special Purpose Materials*, J.R. Davis Ed., ASM International, Materials Park, OH, (1999), p. 903-912.
- [31] Clyne T.W. and Withers P.J., *An Introduction to Metal Matrix Composites*, Ed., Cambridge Solid State Science Series, Cambridge University Press, (1993).